Stitching Grid-wise Atomic Force Microscope Images

Mathias Vestergaard[1], Stefan Bengtson[1], Malte Pedersen[1], Christian Rankl[2] and Thomas B. Moeslund[1]

[1]*Institute of Media Technology, Aalborg University, Aalborg, Denmark*
[2]*AFM R&D, Keysight Technologies, San Fransisco, U.S.A.*

Keywords: Atomic Force Microscopy, RANSAC, Template Matching, Image Stitching.

Abstract: Atomic Force Microscopes (AFM) are able to capture images with a resolution in the nano metre scale. Due to this high resolution, the covered area per image is relatively small, which can be problematic when surveying a sample. A system able to stitch AFM images has been developed to solve this problem. The images exhibit tilt, offset and scanner bow, which are counteracted by subtracting a polynomial from each line. To be able to stitch the images properly template selection is done by analyzing texture and using a voting scheme. Grids of 3x3 images have been successfully leveled and stitched.

1 INTRODUCTION

Atomic Force Microscopes (AFM) are able to create topography images with very high resolution by tracing the surface of a sample, line-by-line with a tiny probe. The resolution of the AFMs is in nanometer scale while conventional optical microscopes, in comparison, are able to achieve a maximum resolution of some hundred nanometers. The limited resolution of optical microscopes is imposed by the way light diffracts (Eaton and West, 2010). The high resolution of the AFM images allows for studies of molecules (Last et al., 2010) and living cells (Johnson, 2011).

However, the improved resolution comes at the cost of increased capturing time, as tracing the surface of a sample, line-by-line, is a slow process which can take several minutes. Another drawback is the decrease in field of view, i.e. the area of the sample contained in a single image. It is therefore not uncommon for the size of the sample to exceed the viewable area of the AFM and to counteract this, most AFMs feature a motorized stage which allows them to automatically capture the sample piece-by-piece.

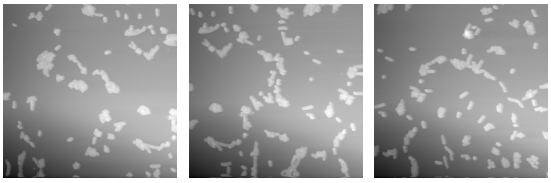

Figure 1: Topography images of bacteria.

The result of this method is a series of images which provides a fragmented view of the sample as seen in Figure 1. The three images are overlapping in the horizontal direction, but it is difficult and tedious to work with this fragmented kind of view. A method to process and stitch the images into a single image without visible seams is therefore wanted.

Because of the high resolution of the AFM even the smallest flaws will be apparent in the images. These flaws complicate the stitching process and require steps to remove potential irregularities. This is necessary as the final image, consisting of several isolated images, should have a uniform background.

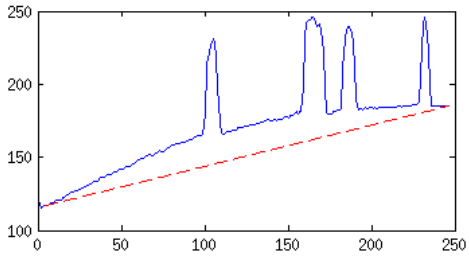

Figure 2: A line from one of the bacteria images. The red line is added to visualize the tilt and scanner bow.

It is difficult to place the sample with enough precision to ensure a horizontally leveled surface and this results in a visible tilt, where the images are darker on one side. An example can be seen in Figure 2, which illustrates a horizontal line taken from one of the bacteria images. The tilt can be seen as the red dashed

Vestergaard, M., Bengtson, S., Pedersen, M., Rankl, C. and Moeslund, T.
Stitching Grid-wise Atomic Force Microscope Images.
DOI: 10.5220/0005716501100117
In *Proceedings of the 11th Joint Conference on Computer Vision, Imaging and Computer Graphics Theory and Applications (VISIGRAPP 2016) - Volume 3: VISAPP*, pages 112-119
ISBN: 978-989-758-175-5

line, which is more or less the same within a specific sample, but may vary from one sample to another.

Most AFMs have only one moving part which is a piezoelectric block that can be placed either beneath or above the sample. This block is controlled by applying current to the sides, which results in a movement pattern similar to that of a pendulum, see Figure 3.

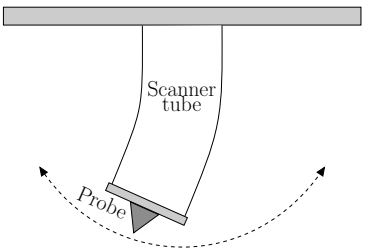

Figure 3: Illustration of the bow is created when a piezoelectric scanner tube is used to move the probe.

This is especially clear in images where the piezoelectric block is forced to approach its maximum range. A phenomenon occurs where an even surface appears to bow and the intensity near the edge of the image is lower than at the center. This bow can be observed in Figure 2.

Beside scanner bow and tilt another problem can occur where some of the objects move or change shape between the capturing of two adjacent images. This can happen if the sample consists of living organisms where movement creates a difficulty in finding the right blending. The same object can end up having two different positions, relative to the rest of the image, if it has moved. In worst case scenarios objects are totally missing as seen in Figure 4.

Figure 4: Two subimages showing the same area of a sample. The subimages are taken from the overlapping part of two images.

2 APPROACH

The proposed solution contains four modules as illustrated in Figure 5. The boxes symbolize the modules which are: Preprocessing, Feature Extraction, Recognition and Post Processing. Between the modules are arrows which represent the way of the workflow. These modules will be described in the following sections.

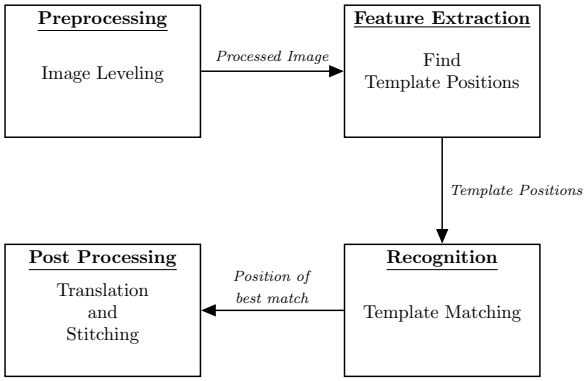

Figure 5: The overall design of the proposed solution.

2.1 Image Leveling

The objective of the leveling process is to remove scanner bow, tilt and offset, while preserving the objects in the images. Traditional image processing techniques are possible solutions, such as the rolling ball algorithm (Lundtoft, 2014).

However, this approach does not account for the characteristics of the artifacts. Namely how they can be described as 2nd order polynomials acquired in a line-by-line pattern.

A common method to level AFM images is therefore to fit and then subtract a polynomial line-by-line for the entire image (Eaton and West, 2010). When fitting the polynomial it is important to exclude the objects to avoid overcompensation which could result in new artifacts (Figure 6).

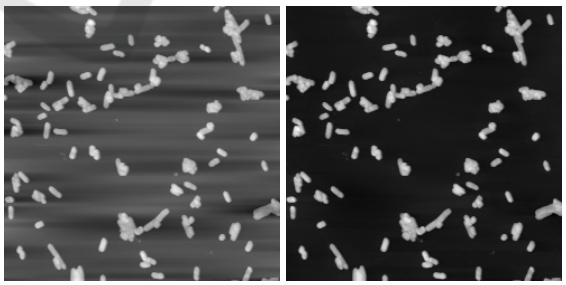

(a) Objects not excluded. (b) Objects excluded.

Figure 6: The same image leveled with and without object exclusion.

Some approaches rely on manual selection of objects to exclude (Eaton and West, 2010), which is very labour intensive and not useful when dealing with a lot of images. Another approach is to use K-means clustering to identify objects in every line (Pan, 2014) (Tsaftaris et al., 2008).

2.1.1 Leveling Algorithm

The developed leveling algorithm expands upon the idea of line-by-line leveling by introducing a new way of automatically excluding objects through the use of RANSAC (Random Sample Consensus) (Fischler and Bolles, 1980). RANSAC is suitable as it is able to estimate parameters of a given model (in this case a 1st or 2nd order polynomial) from a data set (a line from the image) contaminated with outliers (objects). RANSAC basically works by repeatedly making guesses at a solution based on n randomly selected initial points, where n is the minimum number of points required to determine the parameters of the model. Each solution is then evaluated and compared against the current best guess, yielding the best guess as the solution in the end.

RANSAC is therefore non-deterministic and its success depends on the number of iterations k which RANSAC is allowed to execute. k can be determined theoretically based on two assumptions:

The solution is considered decent if:

- All the n initial points are inliers, i.e. part of the polynomial to be removed.
- The n initial points are not closely grouped together, which is evident be contemplating e.g. 2nd order polynomials.

For the sake of simplicity, the number of data points is divided into n evenly sized intervals and the n initial points are considered to be appropriately spaced if each resides in an interval of its own.

Hence, the probability of never reaching a decent solution out of k iterations is given by:

$$P(bad) = (1 - P(in)^n \times P(spaced))^k \quad (1)$$

where $P(in)$ is the probability of a point being an inlier and $P(spaced)$ is the probability of the n points being appropriately spaced, i.e. $P(spaced) = (1/n)^n$. The probability of reaching a decent solution $P(decent)$ out of k iterations must then be given by:

$$1 - P(decent) = (1 - P(in)^n \times (1/n)^n)^k \quad (2)$$

from where k can be isolated:

$$k = \frac{log(1 - P(decent))}{log(1 - P(in)^n \times (1/n)^n)} \quad (3)$$

Considering a scenario with 50% outliers, i.e. $P(in) = 0.50$, and it would take:

$$k = \frac{log(1 - 0.999)}{log(1 - 0.50^3 \times (1/3)^3)} \approx 1488 \quad (4)$$

iterations to find a decent solution with a probability of $P(decent) = 99.9\%$ when using $n = 3$ initial points, which is sufficient for a 2nd order polynomial.

Another solution could be to divide each line into n evenly sized intervals and then randomly choose one point from each interval as the n initial point. This would reduce the number of iterations k to:

$$k = \frac{log(1 - P(decent))}{log(1 - P(in)^n)} \quad (5)$$

as it is no longer necessary to check the spacing between the points, i.e. take $P(spaced)$ into account.

However, this method was found to be inconsistent during tests on real data, as it would repeatedly fail at images with un-evenly distributed outliers, where the majority of outliers would reside in one of the fixed intervals. The idea of using fixed intervals was therefore discarded.

2.1.2 Performance Considerations

A runtime test of a generic RANSAC algorithm is performed to determine whether the $k = 1488$ from Equation 4 is realistic. The algorithm is implemented in C++ and is performed on a laptop with a P8600 @ 2.4GHz CPU. On average (100 repetitions) it took 0.88 seconds to execute the algorithm. Hence, it would take 3 minutes and 45 seconds to apply RANSAC on each horizontal line in a relatively small image of 256×256 pixels, which is not acceptable.

In order to reduce runtime, RANSAC is only used to exclude objects in the first line of the image. In the following lines, the exclusion of objects is achieved by ignoring every point x in the line $l(x)$ which is not within a fixed threshold t from the polynomial $p(x)_{latest}$ found in the previous line. I.e. only points which fulfils

$$t^2 > (p(x)_{latest} - l(x))^2 \quad (6)$$

are used when fitting the polynomial to be subtracted in every line, apart from the first line where RANSAC is used.

2.1.3 Final Leveling Algorithm

The final leveling algorithm is as follows:

1. Fit a polynomial $p(x)_{latest}$ to the first line l_1 in the AFM image using RANSAC.
2. Find inliers in the next line based on $p(x)_{latest}$ and a fixed threshold t.
3. Fit a polynomial to the found inliers and subtract the found polynomial from the current line.

4. Overwrite $p(x)_{latest}$ with the polynomial just found.
5. Repeat step 2-4 until all lines have been processed in the AFM image.

The developed leveling algorithm does well when the percentage of background is noticeably larger than the object percentage (Figure 7).

The leveled images will however start to exhibit an offset in height when the object percentage approaches or exceeds 50% (Figure 8). This issue originates in the initial step of the algorithm, where RANSAC might mistakenly fit a polynomial to the top of the objects instead of the background.

The above issue can be detected by comparing the mean of the current line μ_{line} with the mean of the fitted polynomial μ_{poly}. The polynomial is then considered to be fitted correctly if:

$$\mu_{line} > \mu_{poly} \tag{7}$$

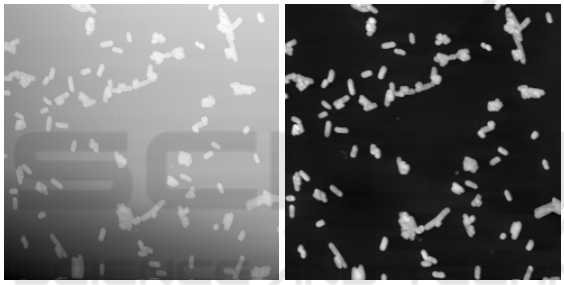

(a) Original image. (b) Leveled image.

Figure 7: Leveling of image with a high background percentage.

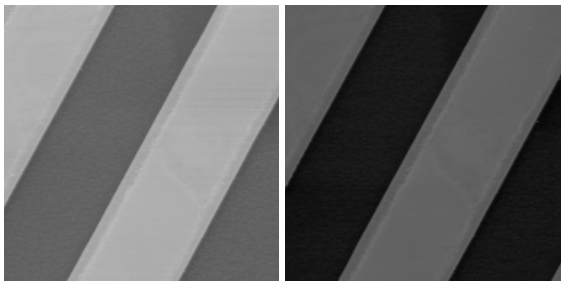

(a) First image. (b) Second image.

Figure 8: Two adjacent images of SiO_2 stripes after leveling. The difference in intensity is caused by the height offset between the images.

The correct polynomial can be found by fitting a polynomial to the outliers, instead of the inliers. This sanity check and correction are easily executed at the end of the developed leveling algorithm.
The average processing time of the developed leveling algorithm, including the above sanity check, is found to be roughly 1 second (see Table 1). This is deemed acceptable considering the time it takes to capture each AFM image (several minutes).

The test was performed on a laptop with a P8600 @ 2.4GHz CPU with datasets containing 9 images each. The bacteria and SiO_2 stripes datasets contains images with a resolution of 256 x 256 pixels, while the bacteria HQ dataset contains images of 512 x 512 pixels. Hence the noticeable difference in runtime.

Table 1: Runtime test of the developed leveling algorithm. Number of iterations is fixed at $k = 1488$.

	Runtime (seconds)		
Dataset	min	avg	max
Bacteria	0.84	0.92	0.95
Bacteria HQ	1.32	1.43	1.49
SiO_2 stripes	0.77	0.81	0.83

2.2 Estimating Translation

A prerequisite for stitching images is the knowledge of how they are related, in this case translation, due to the nature of how the images are acquired using the motorized stage in the AFM. As only translation is present, it is possible to express the relation between two adjacent AFM images as:

$$\begin{bmatrix} x_1 \\ y_1 \end{bmatrix} + \begin{bmatrix} x_{shift} \\ y_{shift} \end{bmatrix} = \begin{bmatrix} x_2 \\ y_2 \end{bmatrix} \tag{8}$$

where $[x_1\ y_1]^T$ is the position of an arbitrary object in image 1, $[x_2\ y_2]^T$ is the position of the corresponding object in image 2 and $[x_{shift}\ y_{shift}]^T$ is the translation. If the position for an object pair (i.e. $[x_1\ y_1]^T$ and $[x_2\ y_2]^T$) is known for a pair of images, it is possible to calculate $[x_{shift}\ y_{shift}]^T$, i.e. the translation between these images.

SIFT (Scale-invariant Feature Transform) (Lowe, 1999) is often used to identify object pairs, when stitching images with varying scale or rotation, e.g. creating panorama images (Brown and Lowe, 2007). However, complications such as scale and rotation are not an issue in the AFM images, which is why a simpler approach is chosen in the form of template matching.

2.2.1 Template Extraction

Some AFM images contain only a small amount of objects and the probability of choosing a region consisting of background is therefore relatively large if no precautions are taken. Templates taken from such regions are difficult to recognize and a solution for finding usable template positions is therefore needed

to ensure that the matching-process has the best conditions.

Good templates are defined as templates containing a high level of texture. In this work we define texture as a region with strong vertical and horizontal edges measured by a Sobel filter. The gradient magnitude found using this filter does not help determine whether a template is unique, but gives an indication of the proportion of the edges contained within. A high level of texture is nevertheless found to be associated with uniqueness and further filtering is not considered necessary.

2.2.2 Template Matching

Normalized Cross Correlation (NCC) (Briechle and Hanebeck, 2001) is used to match the templates, as the AFM images are only exposed to translation. The templates will be extracted from one image and correlated with another (the reference image). NCC is chosen over basic correlation to increase the probability of a successful match even if the leveling does not succeed.

The NCC is given by

$$cos(v) = \frac{A_p \bullet T}{||A_p||\ ||T||} \tag{9}$$

where v is the angle between the template T and the image patch A_p of the reference image A.

The angle v is an expression for the match rate between A_p and T, so when $cos(v)$ approaches 1 the similarity increases. The interval of the match rate is $[0;1]$ as the respective images only consist of positive values.

2.2.3 Region of Interest

The overlapping region is selected as the region of interest during the extraction and matching of templates between the two images. Any template matches outside this region must obviously be wrong and should be discarded anyway.

However, it is possible to limit the ROI even further when looking for a template match in image 2. This is due to the grid-like pattern in which the AFM acquires images, resulting in the following assumptions:

1. The translation between two adjacent images only changes drastically in one direction. I.e. translation in either the horizontal or vertical direction is always negligible or not present at all.
2. The translation is roughly the same between all adjacent images.

From *assumption* 1 the ROI can be limited to either a horizontal or vertical slice (Figure 9) when only the orientation of the two images are known (i.e. image 1 is to the left of image 2).

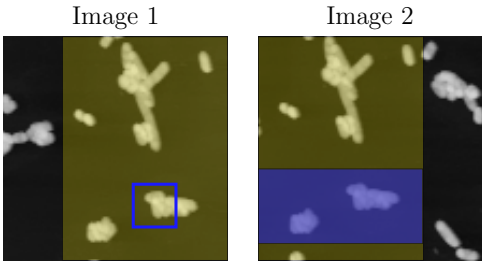

Figure 9: The highlighted area is the overlapping region, the blue square is the template and the blue area is the ROI in image 2.

If a rough translation is known as well (from a previous image pair) it is possible to estimate where the template match is likely to be found on image 2 due to *assumption* 2 (Figure 10).

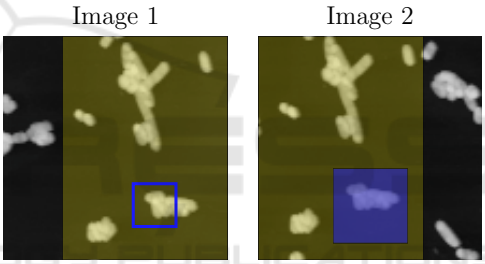

Figure 10: The ROI in image 2 (blue area) is narrowed down even further than in the previous figure.

The translation is therefore estimated as follows:

1. Limit the ROI on both image 1 and 2 to the overlapping region.
2. If a rough translation is known, jump to step 5.
3. Calculate the initial overlap from meta data from the image files and adjust ROI accordingly on image 1.
4. Use *assumption* 1 to limit the ROI on image 2. Skip the next step.
5. Use *assumption* 2 to limit the ROI on image 2.
6. Extract a template T from image 1.
7. Find a match for T in image 2.
8. Calculate translation based on the position of T and the found match.

2.2.4 Multiple Templates

Using a single template match to calculate the translation should be sufficient in theory. However, it is

possible that a match is not correct due to some of the following reasons:

- **Living Samples** - If the sample is alive and moving around, it it possible that a template might not be present in both images.
- **Noise** - Random noise in the images could mess up the template matching and yield a false-positive match.
- **ROI Selection** - The ROI selection might not be spot on and the same template might not be present in the ROIs for both images.

To avoid the impact of these issues, a voting-scheme is utilized to decide which translation to accept. Translation candidates are repeatedly calculated and then allowed to cast a vote. This process stops when a single translation candidate reaches a set number of votes w and wins, or until no more templates can be extracted from image 1. In the latter case, the candidate with the most votes wins.

Each vote cast is weighed:

$$v_{\text{weighted}} = (m_{\text{rate}})^2 \tag{10}$$

where v_{weighted} is the weighted vote and m_{rate} is the similarity measure returned by the NCC in Equation 9. m_{rate} is squared in order to punish translations with a low match rate even further.

2.2.5 Stitching

The last step of the proposed solution is the actual stitching of the images according to the found translations. The images are stitched together two images at a time, first horizontally into rows and then vertically (Figure 11).

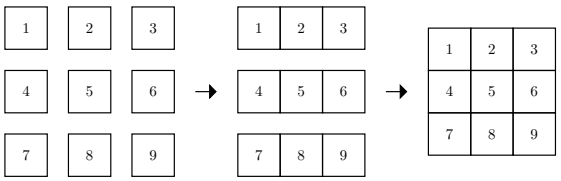

Figure 11: Stitching order.

The stitching order is similar to the order in which the images are captured by the AFM, i.e. row-by-row. This is an intentional choice, as it reduces the impact of movement from living objects. The impact is reduced as the elapsed time between the capturing of e.g. image 1 and 2 is less than the time between image 1 and 4, thereby leaving less time for the objects to move.

Two blending methods have been proposed:

$$P_{mean} = \frac{P_1 + P_2}{2} \tag{11}$$

$$P_{min} = min(P_1, P_2) \tag{12}$$

where P_1 is the respective pixel from the overlapping part of image 1 and P_2 the pixel from image 2.

P_{mean} is used in cases where the trails of movement (ghosting artifacts) should be visible whereas P_{min} is used where these trails are unwanted. A downside of the P_{min} method is that parts of the objects can disappear as the minimum value of the two pixels is used. An example of the two blending methods can be seen in Figure 12, where a slightly wrong translation is used to highlight how the methods behave.

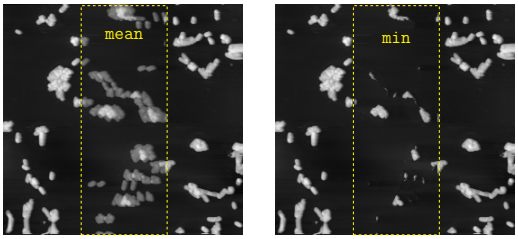

(a) *Mean* blending. (b) *Min* blending.

Figure 12: The two blending methods used on the same overlapping region.

3 RESULTS

A demonstration of how the proposed solution works is illustrated in the bacteria images in Figure 13. The result can be seen in Figure 15 and Figure 16 where the *mean* and *min* blending methods have been used, respectively.

The difference between the two blending methods is not as clear as in the example in Figure 12 although some lines, where the images are stitched, can be seen when the *mean* blending method is used. These lines occur as a result of the missing or moving objects as explained earlier.

The solution is also tested on a dataset exhibiting a high percentage of objects (Figure 14), which is known to cause trouble for the leveling algorithm. The purpose is to test the translation estimation and stitching capabilities when the intensity is not consistent due to the shortcomings of the leveling.

The result of the leveling and stitching process can be seen in Figure 17. It is clear that the leveling algorithm struggles, which is evident due to the many artifacts. Most notable are the sharp seams caused by different intensities and sudden fluctuations in intensity between lines. However, the translation estimation and stitching does appear successful, as the objects agree with the objects found in the original 3x3 image grid.

A runtime test of the entire system is performed on a laptop with a P8600 @ 2.4GHz using grids of

3x3 images. Four different image grids were used, one with a resolution of 512x512 pixels and three of 256x256 pixels. The high resolution grid took 43 seconds to process, while the three lower resolution grids took 13 seconds on average.

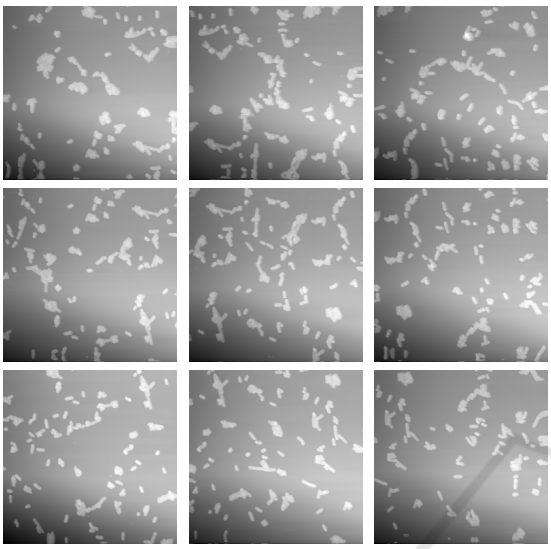

Figure 13: Topography images of bacteria - 3x3 grid.

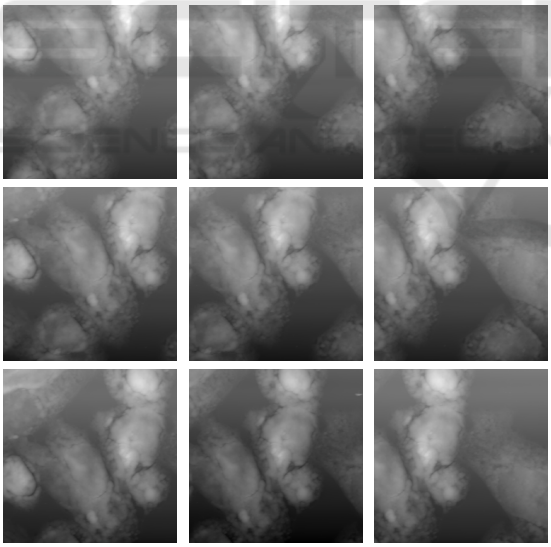

Figure 14: Topography images of CHO cells - 3x3 grid.

4 DISCUSSION

The leveling algorithm starts to fail when the objects occupy a percentage above 90% of each line (Figure 18). This high percentage increases the risk of finding an inferior solution in the initial step where RANSAC is used.

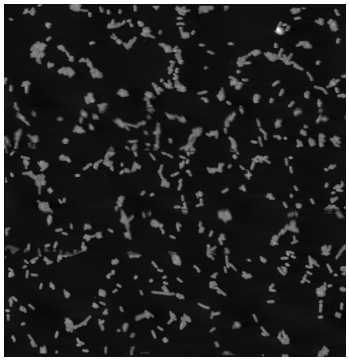

Figure 15: Stitched image of bacteria using the *mean* blending method.

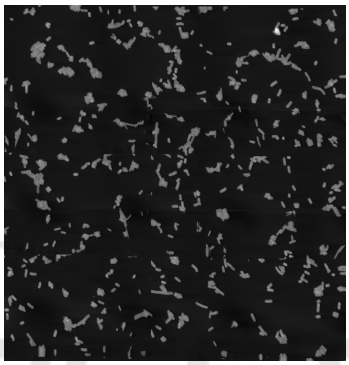

Figure 16: Stitched image of bacteria using the *min* blending method.

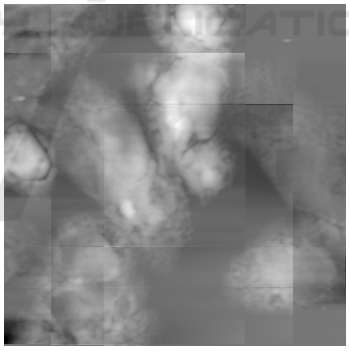

Figure 17: Stitched image of CHO cells using the *min* blending method.

A possible solution could be to apply RANSAC, with fewer iterations, at several random lines in the image, in order to find a line with a decent amount of background. Further tests on diverse datasets could be used to identify the actual limit of the leveling algorithm. Another issue is the impact of the points, which are mistakenly classified as inliers (Figure 19). In images with a relatively low object percentage this is not an issue, as the false inliers will be outweighed by the true inliers when fitting a polynomial.

Reducing the threshold used when identifying in-

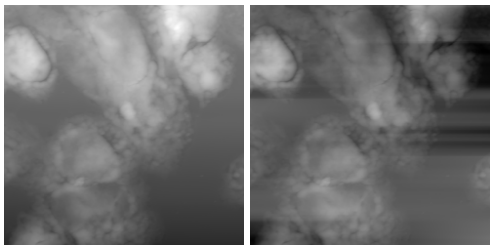

(a) Original image. (b) Leveled image.

Figure 18: Image with a high object percentage.

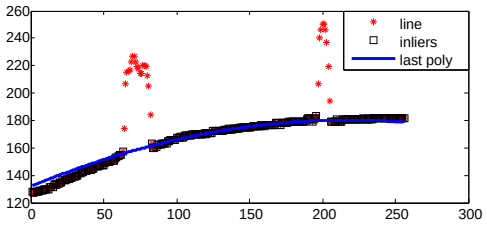

(a) Image 1 - easy to level.

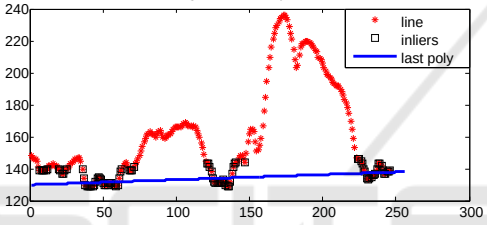

(b) Image 2 - difficult to level.

Figure 19: Example of inlier detection.

liers could be a possible solution to this problem, but it has not been tested. Even if the leveling fails to some degree, the NCC allows for intensity irregularities between the images and is able to find the right translation. An improvement on the template recognition could be to check the uniqueness of extracted templates before attempting to match them.

The choice of the NCC and the region-of-interest selection is based on the assumption that the images are only related through translation. This simple model seems to be a good choice as the images appear to be correctly stitched when disregarding artifacts not caused by the stitching, like failed leveling or disappearing objects.

The mean blending method is able to show how objects have moved between the images and the min method can be used in cases where the overview is more important than the detail. However, a blending method that maintains the original shape of the objects, without ghosting artifacts, such as de-ghosting (M. Uyttendaele and Szeliski, 2001) could improve the output in certain scenarios.

5 CONCLUSION

The proposed solution is able to level and stitch grid-wise captured AFM images with a few limitations as discussed above. It takes between 12-43 seconds for the system to stitch a grid of 3x3 images depending on the size of the images.

The two blending methods work as intended although there are disadvantages to both of them. The decision of which method is the best in a specific situation depends on the user of the system.

REFERENCES

Briechle, K. and Hanebeck, U. D. (2001). Template matching using fast normalized cross correlation. *Optical Pattern Recognition XII*, 4387:95–102.

Brown, M. and Lowe, D. G. (2007). Automatic panoramic image stitching using invariant features. *International Journal of Computer Vision*.

Eaton, P. and West, P. (2010). *Atomic Force Microscopy*. Oxford University Press.

Fischler, M. A. and Bolles, R. C. (1980). Random sample consensus: A paradigm for model fitting with applications to image analysis and automated cartography. http://www.dtic.mil/dtic/tr/fulltext/u2/a460585.pdf.

Johnson, W. T. (2011). Imaging cells with the agilent 6000ilm afm.

Last, J. A. et al. (2010). The applications of atomic force microscopy to vision science. *Invest Ophthalmol Vis Sci*, 51:6083–6094.

Lowe, D. G. (1999). Object recognition from local scale-invariant features. *The Proceedings of the Seventh IEEE International Conference on Computer Vision*.

Lundtoft, D. H. (2014). Internship report from keysight technologies. Technical report, Aalborg University.

M. Uyttendaele, A. E. and Szeliski, R. (2001). Eliminating ghosting and exposure artifacts in image mosaics. *Computer Vision and Pattern Recognition*, pages 509–516.

Pan, X. (2014). Processing and feature analysis of atomic force microscopy images. Master's thesis, Missouri University of Science and Technology.

Tsaftaris, S. A. et al. (2008). Automated line flattening of atomic force microscopy images. Master's thesis, Northwestern University.